

deduced from the systematics for the beta-ray transition of  $2- \rightarrow 2+$ .<sup>8</sup> This fact is consistent with the results of the angular correlation measurement<sup>4,5</sup> which assigned  $2+$  and  $2+$  for the second and third excited levels, respectively.

The 2.5 percent branching ratio and 5.6  $\log ft$  value are obtained for the fourth beta-ray component which is assumed to decay to the third excited level. Since the gamma ray going to ground state was not observed,

<sup>8</sup> R. W. King and D. C. Peaslee, Phys. Rev. **94**, 1284 (1954).

the spin value of  $1+$  and  $2+$  may not be assigned to this level. The most probable spin value may be  $3+$ . Then this beta component has the first forbidden characteristics of  $\Delta I=1$ ; yes. But the assignment of  $3-$  cannot be excluded. Figure 8 presents a decay scheme including all data obtained in the present work.

Support by grants from the Ohio State University Research Foundation through the Graduate School and from the Ohio State University Development Fund are gratefully acknowledged by the authors.

### Interaction of 4.1-Mev Neutrons with Nuclei\*

M. WALT AND J. R. BEYSTER

University of California, Los Alamos Scientific Laboratory, Los Alamos, New Mexico

(Received December 7, 1954)

The differential cross sections for elastic scattering of 4.1-Mev neutrons by Be, C, Al, Ti, Fe, Zn, Zr, Cd, Sn, Ta, W, Au, Pb, and Bi were measured using a biased scintillation detector with thresholds at about 2.0, 2.6, and 3.2 Mev. Multiple scattering corrections were made by an approximate method, the accuracy of which was investigated by Monte Carlo calculations. Inelastic collision cross sections and elastic transport cross sections were computed from the data. The experimental results are compared with theoretical cross sections calculated using the complex square-well potential of Feshbach, Porter, and Weisskopf.

#### I. INTRODUCTION

MEASUREMENTS of angular distributions for scattering of fast neutrons have been performed by many investigators over a wide range of energies.<sup>1-7</sup> In many of these experiments the angular distributions for elements with almost the same atomic weight were observed to have similar shapes. This fact suggests that in the continuum region, where the experimental quantities represent averages over many resonances, the interaction of neutrons with nuclei can be understood in terms of a model employing parameters which vary slowly with atomic weight. In the continuum

region the total cross section can be represented as a sum of the cross sections for elastic scattering and for reactions.

$$\bar{\sigma}_t = \bar{\sigma}_{el} + \bar{\sigma}_r.$$

It has been shown that the elastic scattering cross section can be decomposed into a shape-elastic term and a compound-elastic term.<sup>8,9</sup>

$$\bar{\sigma}_{el} = \sigma_{se} + \sigma_{ce}.$$

This division of the elastic cross section can be interpreted in a simple fashion. The shape-elastic term  $\sigma_{se}$  represents elastic scattering which does not involve compound nucleus formation, and the compound elastic term  $\sigma_{ce}$  denotes elastic scattering produced by the decay of the compound nucleus through the entrance channel. The reaction term  $\bar{\sigma}_r$  indicates a true reaction process such as  $(n,p)$ ,  $(n,\gamma)$ ,  $(n,n')$  etc. Hence, the sum

$$\bar{\sigma}_r + \sigma_{ce} = \sigma_c$$

gives the cross section for compound nucleus formation.

Recently Feshbach, Porter, and Weisskopf<sup>8,10</sup> have proposed a nuclear model which gives reasonable agreement with measured total neutron cross sections at energies from about 0.1 to 3 Mev and with the differential elastic scattering cross sections at 1 Mev.

<sup>8</sup> Feshbach, Porter, and Weisskopf, Phys. Rev. **96**, 448 (1954).

<sup>9</sup> R. G. Thomas, Phys. Rev. **97**, 224 (1955).

<sup>10</sup> Feshbach, Porter, and Weisskopf, Phys. Rev. **90**, 166 (1953); Atomic Energy Commission Report NYO-3076, 1953 (unpublished).

\* Work performed under the auspices of the U. S. Atomic Energy Commission.

<sup>1</sup> Amaldi, Bocciarelli, Cacciapuoti, and Trabacchi, Nuovo cimento **3**, 203 (1946). These authors measured elastic scattering of 14-Mev neutrons by Pb.

<sup>2</sup> E. T. Journey and C. W. Zabel, Phys. Rev. **86**, 594(A) (1952). Angular distribution of fission spectrum neutrons scattered from many elements were measured using threshold detectors.

<sup>3</sup> Baldinger, Huber, Ricamo *et al.*, Helv. Phys. Acta **25**, 142, 435, 444, 447 (1952). Elastic scattering of neutrons by several light elements was measured at many energies up to 4 Mev.

<sup>4</sup> W. D. Whitehead and S. C. Snowden, Phys. Rev. **92**, 114 (1953); **94**, 1267 (1954). Scattering of 3.7-Mev neutrons by six elements was measured.

<sup>5</sup> M. Walt and H. H. Barschall, Phys. Rev. **93**, 1062 (1953). Elastic scattering of 1-Mev neutrons by 28 intermediate and heavy elements was measured.

<sup>6</sup> J. H. Coon (to be published). Elastic scattering of 14-Mev neutrons was measured for five elements.

<sup>7</sup> A. Langsdorf (private communication). Total scattering of neutrons by several elements was measured for many energies up to about 1.5-Mev; Willard, Bair, and Kington (to be published). Elastic scattering of neutrons by several light elements was measured at energies up to 1.5 Mev.

This theory represents the nucleus by a complex square-well potential of the form

$$\begin{aligned} V &= -V_0(1+i\zeta), & r < R \\ V &= 0, & r > R \end{aligned}$$

where  $R$  is the nuclear radius. The parameters which best fit the total cross section data<sup>8,11</sup> are a well depth  $V_0=42$  Mev, an absorption parameter  $\zeta=0.03$ , and a nuclear radius  $R=1.45A^{1/3}\times 10^{-13}$  cm where  $A$  is the number of nucleons in the nucleus. However, several discrepancies of detail do occur between theory and experiment. The measured inelastic collision cross sections at 1 Mev are in some cases much larger than the calculated cross sections for compound nucleus formation. Also, the differential cross sections for elastic scattering of 1-Mev neutrons differ slightly from those predicted by the theory. For example, the secondary maximum which appears at about  $110^\circ$  for elements of atomic weight near 200 occurs at about  $A=180$  in the theory.

The comparison of theory with experiment at 1 Mev is complicated by the fact that at this low energy there are few levels in the residual nucleus available for inelastic scattering. Thus, the compound nucleus has an excellent chance to decay by the entrance channel, producing compound-elastic scattering. Since compound-elastic scattering is experimentally indistinguishable from the shape-elastic scattering, the measured elastic scattering cross sections are composed of an unknown mixture of the compound-elastic and shape-elastic scattering cross sections. By using a higher bombarding energy so that more levels are available for inelastic scattering, this complication can be lessened somewhat. It was therefore decided, as a further test of the theory, to measure the differential elastic scattering cross sections for a number of elements at an energy high enough to avoid the ambiguities introduced by the presence of considerable compound-elastic scattering. An energy of about 4 Mev was chosen because neutrons of this energy could conveniently be produced by the  $H^3(p,n)He^3$  reaction and because all but the lightest elements have several excited states below this energy.

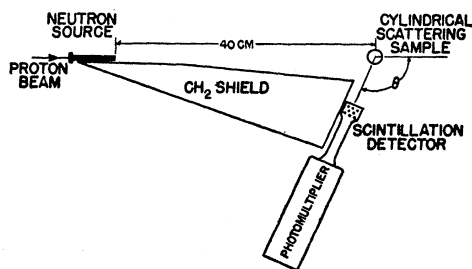


FIG. 1. Top view of experimental arrangement.

<sup>11</sup> R. K. Adair, Phys. Rev. 94, 737 (1954).

## II. EQUIPMENT AND EXPERIMENTAL PROCEDURE

The geometry of the experimental arrangement is shown in Fig. 1. Neutrons produced at the source were scattered by a cylindrical sample of the element being investigated and the intensity of the scattered beam was measured as a function of the angle  $\theta$  by an energy sensitive counter. The detector was shielded from the neutron source by polyethylene wedges.

As described previously,<sup>5</sup> the differential cross sections, subject to several corrections, are given by the formula

$$\sigma(\theta) = (A - B)d^2/CN, \quad (1)$$

where  $A$ ,  $B$ , and  $C$  are the counting rates for a constant neutron source strength observed under three experimental conditions: (A) with the detector at angle  $\theta$  and the scattering cylinder in position; (B) with the detector at angle  $\theta$  and the scattering cylinder removed; and (C) with the detector in the position normally occupied by the scattering sample.  $N$  is the total number of nuclei in the scattering sample, and  $d$  is the distance from the sample to the neutron detector.

The procedure for taking the data was as follows. At each of several angles a number of runs were taken with the scattering sample alternately in place and removed. A run lasted about two minutes, the time being controlled by a current integrator which ended the run when a predetermined proton charge was collected at the target. At frequent intervals the counter was placed in the direct beam in order to measure the counting rate for condition (C). In general the cross sections were measured for values of  $\theta$  equal to  $12.5^\circ$ ,  $20^\circ$ ,  $30^\circ$ ,  $45^\circ$ ,  $60^\circ$ ,  $75^\circ$ ,  $90^\circ$ ,  $105^\circ$ ,  $120^\circ$ ,  $135^\circ$ , and  $150^\circ$ . However, in some cases where the shape of the curve was still in doubt after measurements at these angles had been made, additional angles were used. For angles of  $20^\circ$  or greater the center of the counter was 8.5 cm from the center of the sample. The  $12.5^\circ$  data were obtained with the detector 15 cm from the sample, and the point at  $20^\circ$  was duplicated with the counter at this greater distance. Because of the finite length of the scattering cylinders, the average scattering angle was somewhat different from the angle  $\theta$  of Fig. 1. In all of the data presented on the following pages corrections have been made for this effect.

The distance  $d$  from the scattering sample to the center of the active volume of the detector was measured directly and was also determined by observing the counting rate as a function of distance from the neutron source. The results obtained by these two methods agreed to within 0.5 percent.

The effect of the polyethylene wedges upon the incident neutron flux striking the scattering cylinder was investigated by placing the detector in the position normally occupied by the scattering sample and comparing the counting rate observed with the wedge in position with the counting rate measured with the

polyethylene removed. Repeated measurements indicated that the effect of the wedge on the counting rate was less than 0.5 percent.

Neutrons of 4.1 Mev with an energy spread of about 80 kev were produced by bombarding a tritium gas target with protons from an electrostatic generator. The gas target chamber was six cm in length and was separated from the accelerating tube vacuum system by a 0.0002-inch aluminum foil. The target pressure was maintained at about 60 cm of Hg, and a proton current of 5.0 microamperes was used throughout the experiment. The cylindrical scattering samples were about 6 cm in length and had diameters between 1.27 cm and 2.54 cm depending upon the total cross section of the element and its nuclear density. The diameters were chosen to be about half of one mean free path for neutron collision.

The neutron counter, which is described in more detail elsewhere,<sup>12</sup> was a scintillation detector of a type

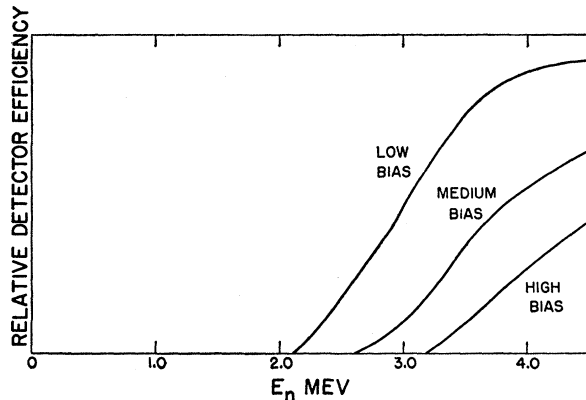


FIG. 2. Relative efficiency of the neutron detector as a function of neutron energy  $E_n$ .

designed for the detection of neutrons in the presence of gamma rays.<sup>13</sup> It consisted of nine plastic phosphor spheres, each 0.1 inch in diameter, separated from each other by about 1 cm of clear quartz. A quartz light pipe coupled the scintillating spheres to a Dumont 6467 photomultiplier. In order to obtain estimates of the energy lost by the neutrons in inelastic collisions the detector was operated at three different biases having detection thresholds at about 2.0, 2.6, and 3.2 Mev. Thus, the presence of neutrons which lost less than 2 Mev in inelastic collisions would be indicated by differences in the cross sections obtained at the three biases. The choice of biases was determined by the experimental conditions. At biases above the highest one used the counting rates were too low; at lower biases the counter was sensitive to gamma rays. The variation in the sensitivity of the detector with neutron energy at the various biases was obtained by comparing

<sup>12</sup> Beyster, Henkel, Nobles, and Kister (to be published).

<sup>13</sup> McCrary, Taylor, and Bonner, Phys. Rev. **94**, 808(A) (1954).

the counting rate of the scintillation detector with the counting rate of an energy insensitive long counter<sup>14,15</sup> at different neutron energies. These results are shown in Fig. 2.

As the analysis of the data required a knowledge of the total cross sections of the fourteen elements studied, transmission measurements were made with the same neutron source and detector used in obtaining the differential cross sections. In-scattering corrections, which amounted to about 0.2 percent of the total cross sections, were computed using the angular distributions obtained in the differential cross section measurements.

### III. ANALYSIS OF THE DATA

Corrections to Eq. (1) were made for the difference in efficiency with which direct and scattered neutrons were detected, for the attenuation of the primary beam in the sample, and for multiple scattering. The procedure for making these corrections has been described elsewhere.<sup>5,16</sup>

Since the angular distributions of elastically scattered 4.1-Mev neutrons were much more anisotropic than were the distributions at 1 Mev, it was decided that the multiple scattering correction procedure used in the previous work at 1-Mev should be tested again using the Monte Carlo method. The experimental data of four elements, C, Fe, Ta, and Pb, were corrected by the method described in references 5 and 16 and the

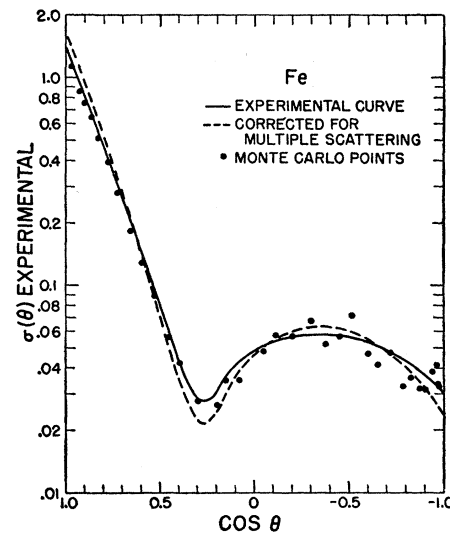


FIG. 3. Multiple scattering correction. The solid line is the experimental curve uncorrected for multiple scattering, and the dotted line shows the experimental curve after the correction for multiple scattering. The circles are the results of a Monte Carlo calculation and represent values which would be measured for an element whose true differential cross section is given by the dotted line.

<sup>14</sup> A. O. Hanson and J. L. McKibben, Phys. Rev. **72**, 673 (1947).

<sup>15</sup> Day, Henkel, Jarvis, Kutarnia, McKibben, Perry, and Smith, Rev. Sci. Instr. **25**, 334 (1954).

<sup>16</sup> M. Walt, Ph.D. Thesis, University of Wisconsin, 1953 (unpublished).

resulting differential elastic cross sections and inelastic collision cross sections were used to determine scattering probabilities for a Monte Carlo calculation using the same geometry as the experimental arrangement of Fig. 1. For each element between 50 000 and 80 000 neutrons were traced through the scattering sample, and the number of scattered neutrons passing through a cylindrical counting band 8.5 cm in radius and 2 cm wide, coaxial with the scattering cylinder, was recorded as a function of the scattering angle  $\theta$ . By comparing the cross sections obtained from the Monte Carlo calculation with the uncorrected experimental cross sections the accuracy of the method of analysis could be estimated. This comparison for Fe is shown in

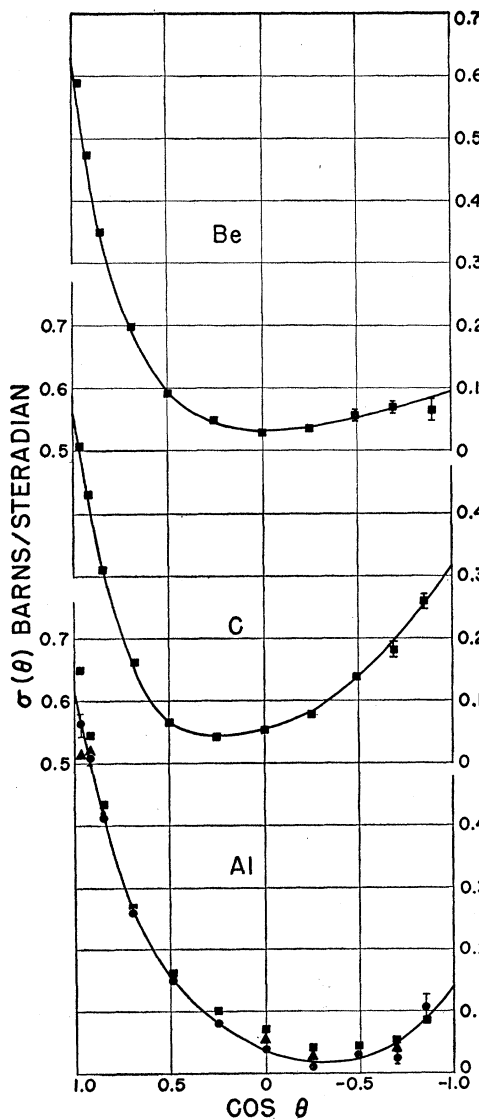


FIG. 4. Differential cross sections in the laboratory system for scattering of 4.1-Mev neutrons by Be, C, and Al. The circles, triangles, and squares denote data taken by the high bias, medium bias, and low bias, respectively.

Fig. 3. The solid line is the experimental curve to which the approximate correction procedure was applied. The dashed curve, which was used as the differential elastic cross section in the Monte Carlo calculation, is the experimental curve after the approximate correction for multiple scattering was made. The solid circles indicate the differential cross sections computed from the Monte Carlo results and represent the cross sections which would have been measured for an element with differential cross section and inelastic collision cross section equal to the Monte Carlo input information. If the approximate correction were exact, the Monte Carlo points would fit the solid curve except for statistical errors resulting from the limited number of neutrons used in the Monte Carlo calculation. The close agreement indicates that any

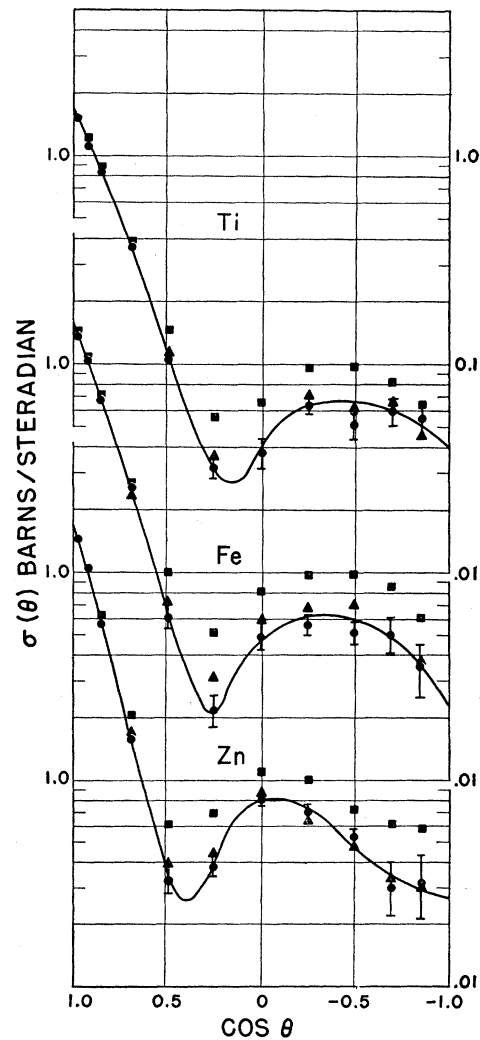


FIG. 5. Differential cross sections in the laboratory system for scattering of 4.1-Mev neutrons by Ti, Fe, and Zn. The circles, triangles, and squares denote data taken by the high bias, medium bias, and low bias, respectively.

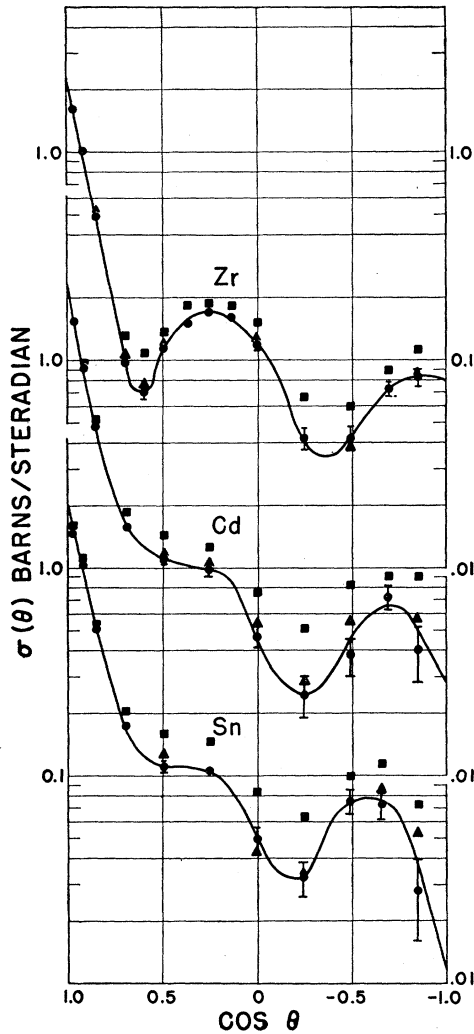


FIG. 6. Differential cross sections in the laboratory system for scattering of 4.1-Mev neutrons by Zr, Cd, and Sn. The circles, triangles, and squares denote data taken by the high bias, medium bias, and low bias, respectively.

errors introduced by the approximate correction procedure are considerably smaller than the errors of the experiment itself. Results similar to that of Fe were obtained for the other three elements tested in this manner.

The inelastic collision cross sections were obtained by means of the equation

$$\sigma_{in} = \sigma_t - \int \sigma(\theta) d\omega,$$

where  $\sigma_t$  is the total cross section obtained by the transmission measurements,  $\sigma(\theta)$  is the differential cross section for elastic scattering, and  $d\omega$  is the solid angle between  $\theta$  and  $\theta + d\theta$ . The elastic transport cross section is also of interest and was obtained from the

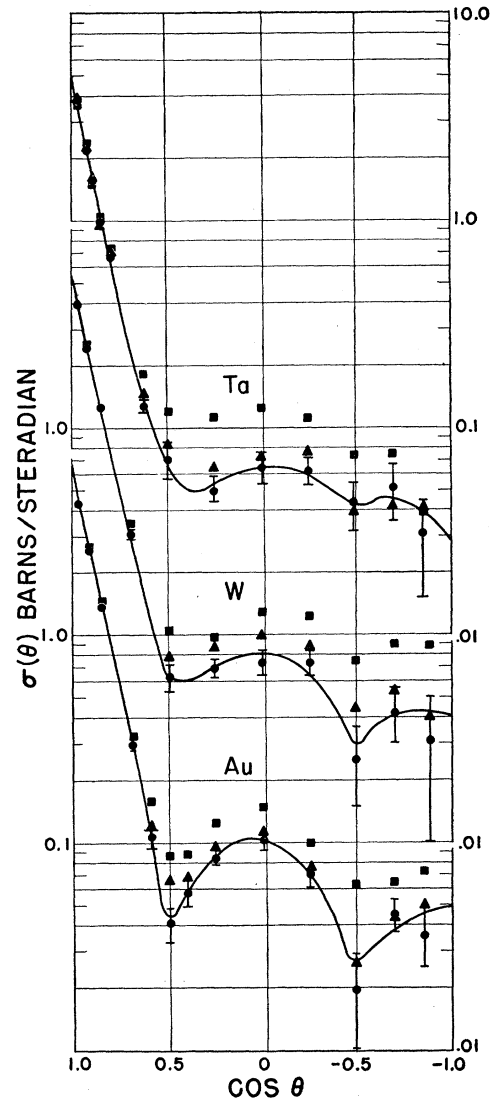


FIG. 7. Differential cross sections in the laboratory system for scattering of 4.1-Mev neutrons by Ta, W, and Au. The circles, triangles, and squares denote data taken by the high bias, medium bias, and low bias, respectively.

definition

$$\sigma_{el\ tr} = \int \sigma(\theta)(1 - \cos\theta) d\omega.$$

#### IV. RESULTS

The differential cross sections for elastic scattering of 4.1-Mev neutrons from Be, C, Al, Ti, Fe, Zn, Zr, Cd, Sn, Ta, W, Au, Pb, and Bi are shown in Figs. 4 to 8. All quantities are in the laboratory system. The circles, triangles, and squares denote data taken with the high bias, medium bias, and low bias respectively. For Be and C, only the cross sections obtained with the lowest bias were plotted since the sensitivity of the detector to neutrons scattered at large angles was too low at the

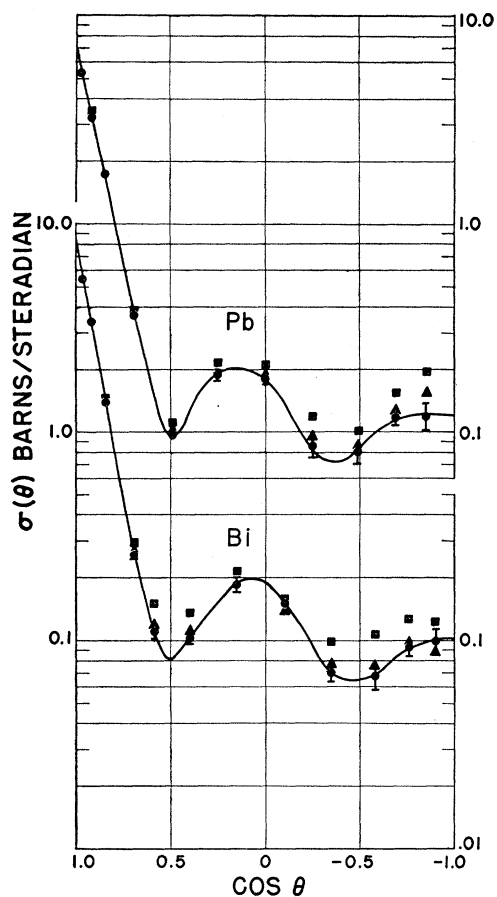


FIG. 8. Differential cross sections in the laboratory system for scattering of 4.1-Mev neutrons by Pb and Bi. The circles, triangles, and squares denote data taken by the high bias, medium bias, and low bias, respectively.

higher biases to give reliable results. At smaller scattering angles there was no significant difference in the results obtained at the three biases. For all elements

TABLE I. The first four columns list the elements investigated and the experimental values of the total cross sections, the inelastic collision cross sections, and the elastic transport cross sections. The next six columns give theoretical values of the total cross sections and the cross sections for compound nucleus formation at three values of the absorption parameter.

Element	Experimental			Theory $V_0=42$ Mev, $R=1.45A^{1/3}\times 10^{-13}$ cm					
	$\sigma_t$	$\sigma_{in}$	$\sigma_{el tr}$	$\zeta=0.03$		$\zeta=0.1$		$\zeta=0.2$	
Be	1.96	$0.6 \pm 0.1$	0.82	1.37	0.49	1.31	0.66	1.19	0.62
C	1.88	$0.08 \pm 0.1$	1.82	0.74	0.26	1.07	0.54	1.21	0.63
Al	2.3	$0.7 \pm 0.2$	0.87	2.39	0.44	2.12	0.74	2.05	0.82
Ti	3.7	$1.2 \pm 0.2$	0.93						
Fe	3.6	$1.5 \pm 0.2$	0.79	3.35	0.50	3.33	0.94	3.20	1.12
Zn	3.7	$1.7 \pm 0.2$	0.74						
Zr	4.1	$1.8 \pm 0.2$	1.13	3.10	0.600	3.58	1.23	3.86	1.44
Cd	4.1	$2.1 \pm 0.2$	0.80						
Sn	4.3	$2.1 \pm 0.2$	0.89	3.81	1.19	4.51	1.68	4.64	1.69
Ta	6.4	$2.7 \pm 0.2$	0.89	7.50	1.75	6.54	2.07	6.17	2.08
W	6.4	$2.4 \pm 0.3$	0.97						
Au	7.1	$2.7 \pm 0.3$	1.02						
Pb	7.8	$1.9 \pm 0.3$	1.83	6.86	1.32	6.78	2.04	6.61	2.21
Bi	7.9	$2.2 \pm 0.3$	1.69						

except Be and C, if points for different biases fell so close together that separate plotting was not possible, the point for the highest bias was used. The curves were drawn through the points obtained with the highest bias, since this bias had better discrimination against inelastically scattered neutrons. The statistical errors for the points taken with the two lower biases were not indicated as sufficient space was not available. In general the statistical errors of the cross sections obtained with the lowest bias were less than half as large as those obtained with the highest bias. Due to the

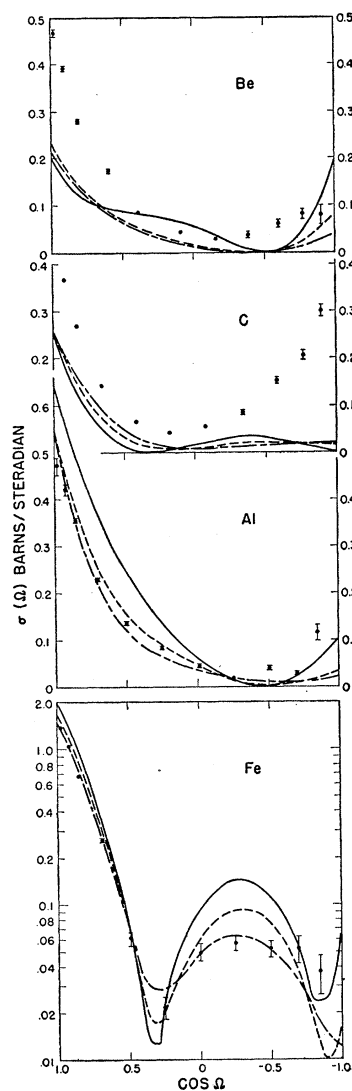


FIG. 9. Comparison of theory and experiment for Be, C, Al, and Fe. The values of the differential shape-elastic scattering cross sections calculated from the complex square-well potential of Feshbach, Porter, and Weisskopf with  $V_0=42$  Mev, and  $R=1.45A^{1/3}\times 10^{-13}$  cm are shown as a function of the center-of-mass scattering angle  $\Omega$ . The solid line, broken line, and dot-and-dash line are for values of  $\zeta=0.03, 0.1,$  and  $0.2,$  respectively. The solid circles are the experimental points. All quantities are in the center-of-mass system.

large statistical errors of the measurements at back angles for some of the heavy elements, the manner in which the curves were drawn was somewhat subjective. For elements such as Ta, W, and Au where the high bias data were very uncertain, the curves were drawn with some consideration to the shapes indicated by the more precise data taken at the lower biases.

Since at the high, medium, and low biases the detector was sensitive to neutrons with energies greater than about 3.2, 2.6, and 2.0 Mev, respectively, the differences between the cross sections obtained with the high bias and those obtained with the lower biases can be attributed to neutrons which were scattered with less than 2.0 Mev loss of energy. These differences were plotted as a function of angle to obtain an estimate of the angular distribution of the inelastically scattered neutrons. In no case did this angular distribution differ significantly from isotropy, although the errors in the differences were large, and a 20 percent effect would probably not have been noticeable. For Be and C there was no measurable difference in the cross sections obtained at the different biases. The inelastic collision cross section of Be is probably due to the  $(n,2n)$  reaction and neither of the resulting neutrons had sufficient energy to be detected at any bias. Carbon showed no bias effect as the inelastic collision cross section is approximately zero at 4.1 Mev.

In Table I are listed the elements studied, the total cross sections, the inelastic collision cross sections, and the elastic transport cross sections. In all cases except Be and C, the inelastic collision cross sections and elastic transport cross sections were computed from the data taken with the highest bias.

V. DISCUSSION OF RESULTS

The most extensive previous angular distribution measurements in this energy region were those performed by Whitehead and Snowden<sup>4</sup> at 3.7 Mev. The general shapes of the angular distribution curves presented here are in reasonable agreement with their results although the absolute values of the differential elastic cross sections of Figs. 4 to 8 are in some cases considerably smaller than their values. In view of the differences in the results obtained at the three biases it is apparent that the measured differential cross sections depend strongly on the ability of the detector to discriminate against inelastically scattered neutrons. Hence, the lack of agreement between the present results and those of reference 4 can possibly be attrib-

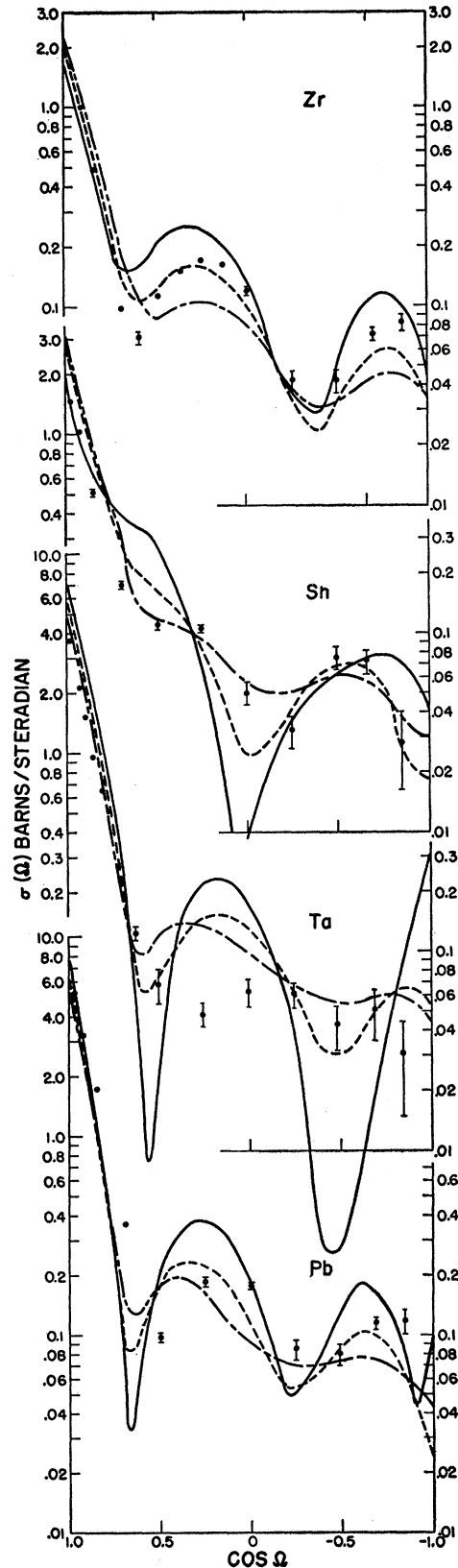


FIG. 10. Comparison of theory and experiment for Zr, Sn, Ta, and Pb. The values of the differential shape-elastic scattering cross sections calculated from the complex square-well potential of Feshbach, Porter, and Weisskopf with  $V_0=42$  Mev, and  $R=1.45A^{1/3}\times 10^{-13}$  cm are shown as a function of the center-of-mass scattering angle  $\Omega$ . The solid line, broken line, and dot-and-dash line are for values of  $\zeta=0.03, 0.1,$  and  $0.2,$  respectively. The solid circles are the experimental points. All quantities are in the center-of-mass system.

uted to the difference in the energy sensitivities of the detectors used in the two experiments.

In the present experiment the variation in the differential cross section with angle is similar for elements with nearly the same atomic weight. This similarity, which has been found in other experiments,<sup>2,4,6</sup> again suggests that the interaction of neutrons with nuclei may be described by a model using parameters which vary slowly with atomic weight.

Comparison of the experimental differential cross sections with those calculated using the continuum theory of Feshbach, Porter, and Weisskopf was made for the representative elements Be, C, Al, Fe, Zr, Sn, Ta, and Pb. For most of the fourteen elements which were measured the compound nucleus formed by bombarding with 4.1-Mev neutrons has sufficient modes of decay to give small probability of compound-elastic scattering. Therefore, the theoretical curves with which the experimental results were compared were those calculated for shape-elastic scattering only. The parameters used in the calculation were  $V_0=42$  Mev,  $R=1.45A^{1/3}\times 10^{-13}$  cm, and  $\zeta=0.03, 0.1,$  and  $0.2$ . This comparison is presented in Figs. 9 and 10. The solid curve, dash curve, and dot-and-dash curve represent the differential shape-elastic cross sections using values of  $\zeta=0.03, 0.1,$  and  $0.2,$  respectively. The circles indicate the experimental points obtained using the highest bias. All quantities are in the center-of-mass system. With the exception of the two lightest elements measured, Be and C, the general features of the experimental data can be accounted for at least qualitatively by the theory. The agreement appears to be best for values of  $\zeta$  between 0.1 and 0.2. The comparison of the cross sections of Be and C with theory is perhaps too severe a test since a statistical theory may not be applicable to cases in which the level spacing of the compound system is on the order of one Mev. Also for small values of  $A$  the character of the curves changes rapidly with small changes of the parameters, and it is possible that minor adjustments of the parameters may produce theoretical curves which will agree with experiment. The assumption of no compound-elastic scattering is certainly not valid for carbon, but as the compound-elastic scattering is symmetric about  $90^\circ$  in the center-of-mass system and is at most about equal to the shape-elastic scattering, the addition of this contribution cannot greatly improve the agreement between theory and experiment.

In Table I the experimental total cross sections and the inelastic collision cross sections are compared with the theoretical total cross sections and cross sections for compound nucleus formation. The cross section for compound nucleus formation is the maximum possible value of the inelastic collision cross section. It is clear that even with an absorption parameter as large as 0.2, the theory cannot account for the large observed inelastic collision cross sections.

Another point of disagreement between the theory and experiment is that the observed maxima and minima of the differential cross section curves for Sn, Ta, and Pb occur at somewhat larger angles than do the calculated maxima and minima. An attempt was made to improve the agreement by decreasing the nuclear radius. Calculations were performed using values of  $R=1.1A^{1/3}\times 10^{-13}, 1.2A^{1/3}\times 10^{-13},$  and  $1.3A^{1/3}\times 10^{-13}$  cm and values of  $V_0$  such that  $R\sqrt{V_0}$  remained constant in order to preserve the agreement in the low energy total cross sections. Although the positions of the maxima and minima were more nearly correct for Pb and Ta using smaller nuclear radii, the computed total cross sections and inelastic collision cross sections were decreased to values quite incompatible with experiment.

The most outstanding disagreement between theory and experiment is in the values of the inelastic collision cross sections. It has been suggested<sup>8</sup> that the sharp boundary of the square-well potential may cause too much reflection at the nuclear surface and hence limit the amount of compound nucleus formation permitted by the theory. Recent calculations performed by Porter<sup>17</sup> substantiate this view.

#### ACKNOWLEDGMENTS

The authors gratefully acknowledge the assistance of L. P. Grant and C. W. Johnstone for the design, construction, and maintenance of the electronic equipment used in the experiment; of H. E. DeWitt and I. J. Cherry for coding the complex square-well scattering problem and performing the calculations on the I.B.M. 701; and of R. L. Bivins, E. D. Cashwell, and C. J. Everett for coding the Monte Carlo multiple scattering problem for the Los Alamos Maniac and performing the calculations. The authors are especially grateful to R. G. Thomas for supervising the complex square-well calculations and for valuable discussions and suggestions during many phases of the work.

<sup>17</sup> C. E. Porter (private communication).